MRS Advances © 2018 Materials Research Society
DOI: 10.1557/adv.2018.512

Vanadium Oxide Thin Film by Aqueous Spray Deposition

Seth Calhoun[1], Rachel Evans[1], Cameron Nickle[1], Isaiah O. Oladeji[2], Justin Cleary[3], Evan M Smith[3], Sayan Chandra[1], Debashis Chanda[1], Robert E. Peale[1]

[1]*Physics Department, University of Central Florida, Orlando, FL, United States.*

[2]*SISOM Thin Films LLC, 1209 W. Gore St. Orlando FL 32805*

[3]*Air Force Research Laboratory, Sensors Directorate, Wright-Patterson AFB, OH, United States.*

ABSTRACT

Vanadium Oxide has application to infrared bolometers due to high temperature coefficient of resistivity (TCR). It has attracted interest for switchable plasmonic devices due to its metal to insulator transition near room temperature. We report here the properties of vanadium oxide deposited by an aqueous spray process. The films have a ropy surface morphology with ~70 nm surface roughness. The polycrystalline phase depends on annealing conditions. The films have TCR of ~2%/deg, which compares well with sputtered films. Only weak evidence is found for an insulator-metal phase transition in these films.

INTRODUCTION

Vanadium Oxide and its different oxidation states have value in opto-electronic devices due to their electrical and optical properties. Semiconducting VO_x with x~2 is well established for infrared bolometers due to its high TCR. VO_2 exhibits a strong resisitivity change with hysteresis that occurs at its semiconductor-metal phase transition near 60 C [2], which is particularly interesting for switchable plasmonic devices. Below this phase transition, the material is semiconducting with a negative TCR. Above, it is metallic with positive TCR. The resistivity drops abruptly by ~100-fold as the temperature passes through the transition from below. The VO_x used for bolometers has the negative room temperature TCR of about -2%/C, but lacks the phase transition [1].

VO_x is typically deposited by vacuum-based methods, which include reactive sputtering of a vanadium target in a partial oxygen environment [3][4], evaporation [5], and pulsed laser deposition [6]. For lower manufacturing costs, a non-vacuum process would be preferable. This paper reports on the properties of vanadium oxide films deposited by an aqueous spray method.

EXPERIMENTAL METHODS

Vanadium oxide (VO_x) films were grown on glass substrates by an aqueous spray method known as Streaming Process for Electrodeless Electrochemical Deposition (SPEED) [10]. The deposition apparatus is manufactured by SISOM Thin Films LLC. Precursors comprised 0.1 M ammonium metavanadate in a mixture of deionized water and organic solvents/ligand. Water (70% by volume) acts as a solvent and as the source of oxygen and the surface-attached OH^- nucleation sites for heterogeneous reaction. The ammonia and organic solvents ethanol, isopropanol, methyl propanol, and other additional reagents serve mainly as complexing agents for V ions. Hydrophilic surfaces readily anchor hydroxyl ions that serve as nucleation sites. The OH^- ions attract positively charged complexes to initiate the electrochemical reaction, without external field or electrodes. The heterogeneous chemical reactions for the growth of VO_2 are

$$[Sub](OH)^- + [VL_n]^{p+(4+)} \rightarrow [Sub]V(OH)^{3+} + (L_n)^p\uparrow \qquad (1)$$

$$[Sub]V(OH)^{+3} + 3OH^- \rightarrow [Sub]VO_2 + 2H_2O\uparrow \qquad (2)$$

where L is the ligand supplied by the organic solvents and other complexing agents, [Sub] the heated substrate, p the charge of the ligand L, and n the number of ligands involved in the V/L coordination. Up arrows indicate decomposition and evaporation of reaction by-products. Substrate temperature must exceed the heterogeneous reaction activation energy and be sufficient to eliminate by-products. Site regeneration follows with the attachment of fresh OH^- to the VO_2, to initiate the next growth cycle. The growth temperature is in the range 300 to 500 °C. Several VO_x films were deposited on different substrates, as described in Table 1. Yellow color is characteristic of V_2O_5 phase.

Conventionally sputtered VO_x and VO_2 films were prepared for comparison. An AJA Phase II J RF sputtering system was used with 99.999% pure Vanadium target in a 2% O_2 in Ar mixture and 400 C substrate temperature.

Films were characterized by scanning electron microscopy (Hitachi S-3500), atomic force microscopy (Digital Instruments multimode SPM), asymmetric out-of-plan x-ray diffraction (PANalytical Empyrean), contact profilometry thickness measurement (Dektak 3), and 4-point probe (Signatone) measurement of temperature-dependent sheet resistance. Resistivity is sheet resistance multiplied by thickness. Temperature dependence of sheet resistance follows $R(T) = R_o\ (1 + \alpha\ \Delta T)$, where $\alpha = d\ln(R)/dT =$

(dR/R)/dT is the TCR. The TCR values are therefore found from the slope of linear fits to ln(R) vs T plots.

Table 1. VO_x Samples grown by SPEED

Sample #	Substrate	Post deposition anneal	Color	Room Temperature Sheet Resistance (Ω/sq)	TCR (%/C)	Resistivity (Ω-cm)
1	glass	60 min, 400 C in air	yellowish	9.2E+08	-2	100000
2	glass	30 min, 400 C in air	mostly gray, some yellow	1.7E+07	-2.2	19000
3	glass	30 min, 450 C in N_2	dark gray	6.6E+04	-2.4	5.9
4	glass	None	uniformly black	2.6E+07	-4	1600
5	glass	30 min, 450 C in N_2	uniformly yellow	8.8E+06	N/A	1800
6	AlN	None	uniformly black	8.8E+07	N/A	8800

RESULTS

Table 1 shows different parameters in the processing and characterization of our samples. The SPEED samples all had thickness in the range 0.6 to 2 μm. In particular, sample 3 had thickness 0.9 μm. Sample 3 is the most semiconductor-like in appearance and resistivity. Samples 3 and 5 had the same annealing conditions but they resulted in different film color and resistivity, implying different oxidation states being formed. SPEED was performed in air using air as the carrier gas. The technique requires a number of spray cycles. The time in between these cycles can be up to a minute to allow the reaction to occur. It was seen that if this time between cycles was too long the sample would turn yellow and post growth annealing in a reducing environment failed to convert it back to its semiconducting state.

Figure 1 (left) presents an SEM image of VO_x sample 3. The ropy surface structure is typical of all samples. This morphology is the same as for TiO_2 samples grown previously by a particular SPEED recipe [8]. In principle, it should be possible to produce VO_x films with a much smoother surface by SPEED [9]. The ropy rings have 2 to 5 μm diameters, which is sufficiently less than LWIR wavelengths that no scattering effects on performance of bolometers made from these high resistivity films is expected.

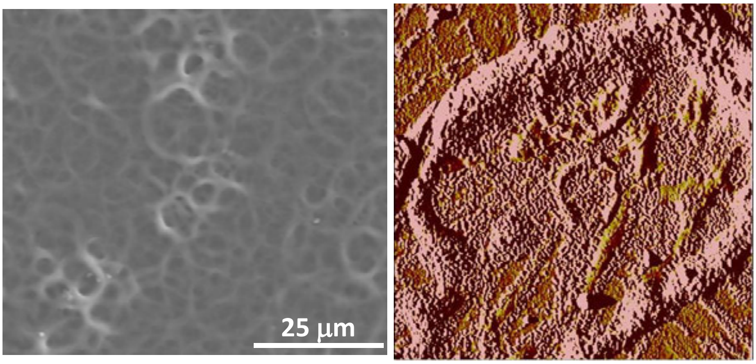

Figure 1 (left). SEM Image of VO_X sample 3. **(right)** 10 µm x 10 µm AFM image of VO_x sample 6.

Figure 1 (right) presents a characteristic AFM image of VO_x sample 6. The average surface roughness was found to be 25 nm, and all AFM images of the surface give comparable results. This value is comparable to reports on other VO_2 polycrystalline films [7]. It is much less than LWIR wavelengths, so that no IR scattering effects will occur for our high resistivity semiconducting VO_x that could impact bolometric sensing applications.

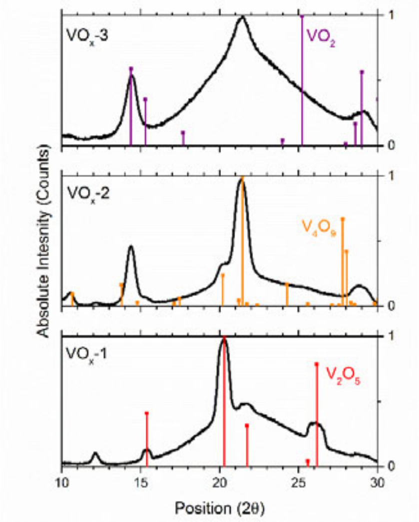

Figure 2. Intensity of XRD of the three VOx samples 1 to 3.

Figure 2 presents x-ray diffraction data of the first three SPEED films. Measured scattering intensity is given by the black curves. Reference data is represented by colored symbols with drop lines. Sample 1 appears to be mainly V_2O_5. The less oxidized phase V_4O_9 becomes dominant in sample 2. Peaks due to VO_2 are present in both samples 2 and 3. Longer anneal in air unsurprisingly increases the oxidation.

Figure 3 compares temperature dependence of sheet resistance (Ω/sq) for conventionally sputtered VO_x and VO_2 films with results for SPEED VO_x sample 3. Sputtered VO_x samples appear to be polycrystalline due to the slight phase transition seen near 55 degrees Celsius. The dependence of sheet resistance on thickness for sputtered films is non-monotonic and is less than expected if the resistivity is the same. The room-temperature resistivity values for the sputtered VO_x films are all comparable to that for the sprayed sample 3. The TCR of the sputtered films near room temperature ranges from -1.7 to -2.1%. The crystalline VO_2 shows the expected phase transition around 65 degrees Celsius with a 400-fold resistance decrease. At the center of the SPEED film, TCR = -1.6%/deg, but at the edge, the higher value -2.4 %/deg is found. This portion shows weak evidence of a phase transition near 55 C. The TCR values from the sprayed film is as promising for bolometer applications as from the sputtered films.

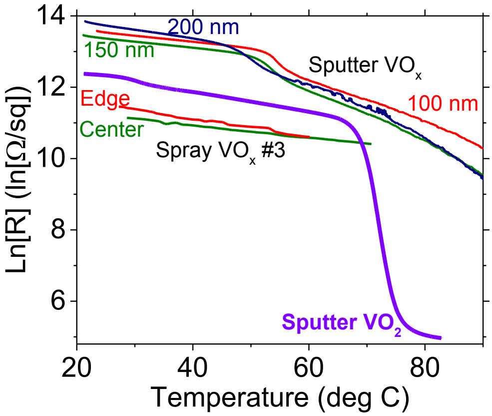

Figure 3. Temperature dependence of sheet resistance for conventionally sputtered VO_x and VO_2 and for sprayed VO_x sample #3.

CONCLUSIONS

Polycrystalline VO_x films were deposited by an aqueous spray technique, which promises low cost manufacturing. The surfaces have ropy ring morphology, though the roughness amplitude is only ~25 nm. The crystalline phase was a mixture of VO_2, V_4O_9, and V_2O_5. The higher oxidation state is found in samples annealed in air. These are yellowish, which is characteristic of vanadium pentoxide. A sample annealed in reducing environment showed evidence of the lower oxidation state VO_2, though such an anneal could not reduce the film back to its grey semiconducting state once it turned yellow. Longer isothermal anneals in air gave higher oxidation state. The effect of differing annealing temperatures in the range 400 – 450 C was unremarkable. To control the oxidation, the spray depositions themselves should be done in a reducing environment with nitrogen carrier gas, and the time between spray cycles should be optimized. All of the samples show a negative TCR near room temperature with value comparable to conventionally sputtered films studied here and elsewhere [2, 11]. Hence, SPEED-grown VO_x would be suitable for room-temperature bolometric applications.

REFRENCES

1. F. Niklaus, C. Vieider, H. Jakobsen, Proc. SPIE 6836 (2007).
2. F.J. Morin, Phys. Rev. Lett. 3, 34 (1959)
3. N. Fieldhouse, S. M. Pursel, M. W. Horn and S. S. N. Bharadwaja, J. Applied Physics D 42, 055408 (2009).
4. J. Cui, D. Da, W. Jiang, Applied Surface Science 133, 225 (1998).
5. G. Chiarello, R. Barberi, A. Amoddeo, L.S. Caputi, E. Colavita, Applied Surface Science 99, 15 (1996).
6. R. T. Rajendra Kumar, B. Karunagaran, D. Mangalaraj, S. K. Narayandass, P. Manoravi, M. Joeseph, V. Gopal, Sensors and Actuators A: Physical 107, 62 (2003).
7. M. Nagashima and H. Wada, J. Crystal Growth 179, 539 (1997).
8. S. F. H. Alhasan, F. Khalilzadeh-Rezaie, R. E. Peale, I. O. Oladeji, MRS Advances 1, 3169 (2016).
9. S. F. H. Alhasan, S. R. Calhoun, H. Abouelkhair, V. C. Lowry, R. E. Peale, I. Rezadad, E. M. Smith, J. W. Cleary, I. O. Oladeji, MRS Advances 3, 255 (2018).
10. R. E. Peale, E. Smith, H. Abouelkhair, I. O. Oladeji, S. Vangala, T. Cooper, G. Grzybowski, F. Khalilzadeh-Rezaie, J. W. Cleary, Opt. Eng. 56, 037109 (2017).
11. E. M. Smith, D. Panjwani, J. Ginn, A. P. Warren, C. Long, P. Figuieredo, C. Smith, J. Nath, J. Perlstein, N. Walter, C. Hirschmugl, R. E. Peale, and D. Shelton, Applied Optics 55, 2071 (2016).